Neurobiology of Disease 37 (2010) 330–338

Contents lists available at ScienceDirect

Neurobiology of Disease

journal homepage: www.elsevier.com/locate/ynbdi

VPS41, a protein involved in lysosomal trafficking, is protective in *Caenorhabditis elegans* and mammalian cellular models of Parkinson's disease

Qingmin Ruan [a], Adam J. Harrington [b], Kim A. Caldwell [a,b], Guy A. Caldwell [a,b], David G. Standaert [a,*]

[a] Center for Neurodegeneration and Experiment Therapeutics, University of Alabama at Birmingham, 1719 6th Ave South, CIRC 516, Birmingham, AL 35294, USA
[b] Department of Biological Sciences, The University of Alabama, Tuscaloosa, Alabama, USA

ARTICLE INFO

Article history:
Received 13 June 2009
Revised 9 October 2009
Accepted 10 October 2009
Available online 20 October 2009

Keyword:
Parkinson's disease
VPS41
alpha-Synuclein
Aggregation
Apoptosis
Mitochondria
6-Hydroxydopamine
Caspase

ABSTRACT

VPS41 is a protein identified as a potential therapeutic target for Parkinson's disease (PD) as a result of a high-throughput RNAi screen in *Caenorhabditis elegans*. VPS41 has a plausible mechanistic link to the pathogenesis of PD, as in yeast it is known to participate in trafficking of proteins to the lysosomal system and several recent lines of evidence have pointed to the importance of lysosomal system dysfunction in the neurotoxicity of alpha-synuclein (α-syn). We found that expression of the human form of VPS41 (hVPS41) prevents dopamine (DA) neuron loss induced by α-syn overexpression and 6-hydroxydopamine (6-OHDA) neurotoxicity in *C. elegans*. In SH-SY5Y neuroblastoma cell lines stably transfected with hVPS41, we determined that presence of this protein conferred protection against the neurotoxins 6-OHDA and rotenone. Overexpression of hVPS41 did not alter the mitochondrial membrane depolarization induced by these neurotoxins. hVPS41 did, however, block downstream events in the apoptotic cascade including activation of caspase-9 and caspase-3, and PARP cleavage. We also observed that hVPS41 reduced the accumulation of insoluble high-molecular weight forms of α-syn in SH-SY5Y cells after treatment with rotenone. These data show that hVPS41 is protective against both α-syn and neurotoxic-mediated injury in invertebrate and cellular models of PD. These protective functions may be related to enhanced clearance of misfolded or aggregated protein, including α-syn. Our studies indicate that hVPS41 may be a useful target for developing therapeutic strategies for human PD.

Introduction

Parkinson's disease (PD) is a disabling neurodegenerative disorder marked by progressive motor dysfunction and characterized by the loss of nigrostriatal dopamine (DA) neurons and cytoplasmic inclusions termed Lewy bodies (Lang and Lozano, 1998; Olanow and Tatton, 1999). While the pathogenesis of PD has not yet been established, previous studies have implicated both genetic as well as environmental contributions. The protein alpha-synuclein (α-syn) appears to have a central role; mutations or overexpression of this protein leads to autosomal dominant PD (Singleton et al., 2003), and accumulation of α-syn is observed even in sporadic cases of PD (Kotzbauer et al., 2004), possibly as a result of impaired protein clearance. No treatment has yet been demonstrated to slow the rate of the neurodegenerative process in PD, and the discovery of potentially protective pathways is a high priority (Yacoubian and Standaert, 2009).

Animal models of PD have been constructed by overexpression of α-syn, and several of these have been used to identify factors that protect against α-syn toxicity. In a recent study, a nematode model of α-syn-induced misfolding and age-dependent DA neurodegeneration was used to screen a candidate list of ~900 starting targets, derived from analysis of proteins or pathways implicated in PD, as well as coexpressed and interacting partners (Hamamichi et al., 2008). From this screen, 20 candidate gene products were identified that, when inhibited, reproducibly led to an enhanced misfolding of human α-syn in worms. In a secondary analysis, select candidates were expressed together with α-syn in *Caenorhabditis elegans* DA neurons, and loss of DA neurons was assessed. One of the most effective neuroprotective proteins identified was VPS41, encoding a conserved vesicular protein necessary for lysosomal biogenesis.

VPS41 was originally identified in yeast as a member of the "class B" proteins involved in trafficking of proteins from the late Golgi to the vacuole (the yeast equivalent of the lysosome) (Bowers and Stevens, 2005). Subsequent work has shown that VPS41 has an unusual role in yeast metabolism, in that it is required for the "ALP" pathway, which bypasses the endosome and carries only a select set of protein cargoes to the vacuole (Rehling et al., 1999). VPS41 has metal ion binding, microtubule binding, RING finger, and AP3 interaction domains (Radisky et al., 1997). It was suggested that the RING-H2 domain associated with a class of intracellular vesicles that originated from the Golgi (McVey Ward et al., 2001).

* Corresponding author. Fax: +1 205 996 6580.
E-mail address: dstandaert@uab.edu (D.G. Standaert).
Available online on ScienceDirect (www.sciencedirect.com).

0969-9961/$ – see front matter © 2009 Elsevier Inc. All rights reserved.
doi:10.1016/j.nbd.2009.10.011

Two isoforms of VPS41 are expressed in humans (McVey Ward et al., 2001), and there is a strong circumstantial case that these proteins may be relevant to α-syn-related disease. Several recent lines of evidence have pointed to the importance of lysosomal system dysfunction in the toxicity of α-syn: the α-syn protein is degraded in part by the lysosomal pathway, under the regulation of the co-chaperone CHIP (Shin et al., 2005); augmentation of the lysososomal enzyme cathepsin D can accelerate the degradation of α-syn (Cullen et al., 2009; Qiao et al., 2008); lysosomal failure has been proposed as a mechanism underlying the age dependence of PD (Chu and Kordower, 2007); modified forms of α-syn can block the chaperone-mediated component of autophagy (Bandhyopadhyay and Cuervo, 2007; Finkbeiner et al., 2006); PARK9, a hereditary form of parkinsonism with dementia, has been linked to a mutation of a lysosomal ATPase (Ramirez et al., 2006) that contributes to α-syn accumulation and manganese toxicity (Gitler et al., 2009); and recently, knockout of the lysosomal protein ATG7 (also identified in the *C. elegans* screen along with VPS41) has been reported to produce a neurodegenerative phenotype (Komatsu et al., 2006). Furthermore, recent studies have described the ability of other vesicular trafficking proteins such as Rab1, Rab3, and Rab8 proteins to mitigate the toxicity of α-syn in animal models of PD (Cooper et al., 2006).

In this study, we show that the functions of VPS41 are evolutionarily conserved, in that overexpression of human VPS41 (hVPS41) in the *C. elegans* model of PD produces protection against both α-syn= and 6-hydroxydopamine (6-OHDA) -induced DA neurodegeneration. Furthermore, we set out to determine whether hVPS41 would have protective effects in mammalian cellular models of PD and to explore the possible mechanism underlying its effect. Stably transfected cell lines were derived from SH-SY5Y neuroblastoma cells and later subjected to several PD-relevant neurotoxins, including rotenone and 6-OHDA. We found that the overexpression of hVPS41 was protective as it reduced the extent of cell death induced by these neurotoxins. Of note, overexpression of hVPS41 failed to alter the mitochondrial membrane depolarization induced by these neurotoxins. However, downstream events in the apoptotic cascade induced by rotenone or 6-OHDA, including caspase-9, caspase-3 activation, and PARP cleavage, were attenuated by hVPS41 overexpression in these cell lines. In addition, we observed that the expression of hVPS41 reduced the accumulation of detergent-insoluble high-molecular weight forms of α-syn, suggesting that modulation of α-syn contributes to its protective actions.

Overall, our data support the hypothesis that hVPS41 represents a potential therapeutic target in PD and that its protective effect is mediated at least in part through modulation of the apoptotic cell death pathway. Furthermore, the protective function of hVPS41 may result from its effect on modulating protein misfolding or aggregation. Our study strongly implicates hVPS41 as a potential target for therapeutic development and intervention to combat PD.

Materials and methods

Generation of transgenic C. elegans

Gateway Technology (Invitrogen) was used to generate expression plasmids, $P_{dat\text{-}1}$::h*vps41 Isoform 1*, $P_{dat\text{-}1}$::h*vps41 Isoform 2*, along with the marker $P_{unc\text{-}54}$::mCherry. These plasmids were injected into the gonads of N2 Bristol *C. elegans* to generate independent stable transgenic lines that were crossed into strains BY200 [$P_{dat\text{-}1}$::GFP] (Nass and Blakely, 2003), which express GFP in the DA neurons without degeneration, and UA44 [*baIn11*; $P_{dat\text{-}1}$:: α-syn, $P_{dat\text{-}1}$::gfp], which coexpresses human α-syn and GFP in the DA neurons and exhibits age-dependent α-syn-induced degeneration. This resulted in 4 independent transgenic worm strains, UA127 [BY200; *baEx98*, $P_{dat\text{-}1}$::h*vps41-1*, $P_{unc\text{-}54}$::mCherry], UA129 [BY200; *baEx99*, $P_{dat\text{-}1}$::h*vps41-2*, $P_{unc\text{-}54}$::mCherry], UA126 [*baIn11*; *baEx98*, $P_{dat\text{-}1}$::h*vps41-1*, $P_{unc\text{-}54}$::mCherry], and UA128 [*baIn11*; *baEx99*, $P_{dat\text{-}1}$::h*vps41-2*, $P_{unc\text{-}54}$::mCherry].

Analysis of DA neurodegeneration in C. elegans

Strains UA126 and UA128 were synchronized, grown at 20 °C, and analyzed at both day 7 and day 10 post-hatching (4- and 7-day-old adults) for protection against α-syn-induced DA neurodegeneration. For each trial, 30 worms were immobilized with 3 mM levamisole and placed on a 2% agarose pad on a microscope slide, where the 6 anterior DA neurons (4 CEP and 2 ADE neurons) were analyzed. In total, 90 worms from each of the 3 independent hVPS41 transgenic lines were analyzed (3 lines × 3 trials of 30 animals/trial = 270 total animals scored). Worms displaying any degenerative changes in the neurons were scored as having degenerating neurons, as previously described (Cao et al., 2005; Hamamichi et al., 2008). Fluorescent microscopy was performed using a Nikon Eclipse E800 epifluorescence microscope equipped with an Endow GFP HYQ filter cube (Chroma Technology, Rockingham, VT), and images were acquired with a Cool Snap CCD camera (Photometrics, Tucson, AZ) driven by MetaMorph software (Molecular Devices, Downington, PA). These data were statistically analyzed by the Student's *t*-test.

Worm strains UA127 and UA129 were treated with 6-OHDA as follows. These worms were synchronized, grown at 25 °C for 35 hours (until late L3 stage), and then treated with 10 mM 6-OHDA containing 2 mM ascorbic acid for 1 hour with gentle agitation every 10 minutes, as previously described (Nass et al., 2002). The worms were then washed and transferred to NGM plates seeded with bacteria (OP50), and DA neurons were scored at 24, 48, and 72 hours post-treatment. DA analysis was performed as described above.

Cell culture and generation of stable cell lines

cDNA clones of hVPS41 (including both isoforms) were obtained from Origene (Rockville, MD) and subcloned into the mammalian expression vector pcDNA 6/myc-His, which has a blasticidin-selectable marker to allow selection for stably transfected cells. DNA constructs were verified by automated sequencing. For stable transfection, SH-SY5Y cells were electroporated with various pcDNA constructs mentioned. Two days after transfection, the cells were maintained with 5 μg/ml blasticidin to select stable transfectants and were then subsequently subcloned. SH-SY5Y cells stably transfected with vector only were used as controls. Cells were selected and maintained on Corning dishes in Dulbecco's modified Eagle's medium (DMEM) supplemented with 5 μg/ml blasticidin, 10% fetal bovine serum, 10 U/ml penicillin, and 100 μg/ml streptomycin. Cells were grown in a humidified atmosphere containing 5% CO_2.

Cell treatment paradigm

Twenty-four hours after plating, cells were transferred to serum-free media and were subjected to designated treatment thereafter. Rotenone or staurosporine was prepared freshly in DMSO, and cells were treated with 0.1–20 μM rotenone (Sigma, St. Louis, MO, USA) or 0.04–1 μM staurosporine (Sigma, St. Louis, MO, USA); the final concentration of DMSO in the media was 0.1%. For 6-OHDA, dilutions of 6-OHDA were made immediately before 6-OHDA addition in 0.1% ascorbic acid and added to fresh cell culture medium to achieve the required concentration. Control cells were treated with 0.1% ascorbic acid under the same conditions.

LDH assay for cell viability

The release of the intracellular enzyme lactate dehydrogenase (LDH) into the medium was used as a quantitative measurement of cell viability. The measurement of LDH was carried out as described previously (Decker and Lohmann-Matthes, 1988).

Immunoblotting

Cells were rinsed in ice-cold phosphate-buffered saline (PBS) and collected in lysis buffer, containing 0.5% NP-40, 150 mM NaCl, 10 mM Tris–HCl (pH 7.4), 1 mM EGTA, 1 mM EDTA, 1 mM phenylmethylsulphonyl fluoride (PMSF), 1 μM okadaic acid, and 10 μg/ml each of aprotinin, leupeptin, and pepstatin. Samples were sonicated on ice for 10 seconds and centrifuged at 16,000× *g* for 10 min. Protein concentrations of supernatants were then determined by the bicinchoninic acid assay (BCA) and samples were diluted to a final concentration of 1 mg/ml with 2×reducing stop buffer (0.25 M Tris–HCl, pH 6.8, 5 mM EDTA, 5 mM EGTA, 25 mM dithiothreitol, 2% SDS, 10% glycerol, and bromophenol blue as the tracking dye). Samples (20 μg of protein) were resolved on 10% or 12.5% SDS–polyacrylamide gels, and transferred to PVDF membrane. Blots were blocked in 5% nonfat dry milk in TBST (20 mM Tris–HCl, pH 7.6, 137 mM NaCl, 0.05% Tween 20) for 1 hour at room temperature. The blots were then incubated with an anti-cleaved caspase-3 polyclonal antibody, or with the anti-cleaved PARP polyclonal antibody in the same buffer overnight at 4°C. The membranes were then washed three times with TBST and incubated with HRP-conjugated secondary antibody for 2 hours at room temperature. The membranes were rinsed three times for 30 min with TBST, followed by four quick rinses with distilled water, and developed with the enhanced chemiluminescence method.

In situ caspase-3 activity

In situ caspase-3 activity was measured using a previously described protocol (Bijur et al., 2000). In brief, 200 μl of assay buffer (20 mM HEPES, pH 7.5, 10% glycerol, and 2 mM dithiothreitol) containing the peptide substrate for caspase-3 (AC-DEVD-AMC) was added to each well (final concentration of 25 ng/μl) of a 96-well clear bottom plate (Corning). Cell lysate (20 μg of protein) was added to start the reaction. Duplicate or triplicate measurements were performed for each sample. Background fluorescence was measured in wells containing assay buffer, substrate, and lysis buffer only. Assay plates were incubated at 37°C for 2 hours, and fluorescence was measured on a fluorescence plate reader set at 360 nm excitation and 460 nm emission.

Detection of the mitochondrial membrane potential ($\Delta\psi_m$)

$\Delta\psi_m$ was analyzed using 5,5,6,6-tetrachloro-1,1,3,3-tetraethylbenzimidazolyl-carbocyanine iodide (JC-1), a lipophilic cationic fluorescence dye. JC-1 is driven into mitochondria in a membrane potential-dependent manner. At high mitochondrial membrane potentials, JC-1 accumulates sufficiently in the mitochondria to form aggregates that fluoresce red. At lower mitochondrial potentials, less dye enters mitochondria resulting in monomers that fluoresce green (Nicholls and Ward, 2000; Smiley et al., 1991). For these studies, cells were grown on 24-well plates. After treatment, cells were incubated with 5 μg/ml JC-1 for 30 min at room temperature in the dark. Then cells were washed twice with PBS and fluorescence was measured on a fluorescence plate reader set at 485 nm excitation and 528 nm emission for green monomer or 530 nm excitation and 590 nm emission for red aggregate.

α-Syn solubility analysis

This experiment was carried out as previously described with minor modification (Cantuti-Castelvetri et al., 2005). Briefly, cell lysates were collected in cold lysis buffer (50 mM Tris–HCl pH 7.4, 175 mM NaCl, 5 mM EDTA pH 7.0, 1 mM PMSF, 1 μM okadaic acid, and 10 μg/ml each of aprotinin, leupeptin, and pepstatin) and sonicated for 10 seconds to generate total cell lysates. These lysates were divided into Triton X-100 soluble and insoluble fractions by adding Triton X-100 to total cell lysates (final concentration of 1%) and incubated for 30 minutes on ice followed by centrifugation (15,000×*g*, 15 minutes, 4 °C). The supernatant was designated as the Triton X-100 soluble fraction. The pellet was dissolved in lysis buffer containing 2% SDS and sonicated for 10 seconds. This was designated the Triton X-100 insoluble fraction. Forty micrograms of Triton-insoluble fraction or 3 μg of Triton-soluble fraction was loaded onto 8% to 15% SDS–polyacrylamide gels and subsequently transferred to nitrocellulose membrane. After blocking, blots were subjected to anti-α-syn antibody (BD Transduction Lab, San Jose, CA) overnight at 4 °C and subsequently developed as described previously.

Results

Expression of hVPS41 rescues DA neuron loss induced by α-syn overexpression and 6-OHDA neurotoxicity in C. elegans

Our prior study in *C. elegans* demonstrated that inhibition of the worm ortholog of VPS41 (the *C. elegans* VPS41 gene product) by RNAi increased the aggregation of α-syn and that overexpression of this protein protected nematode dopamine (DA) neurons against α-syn-induced degeneration (Hamamichi et al., 2008). As a first step, we sought to confirm that hVPS41 shared these neuroprotective properties in the *C. elegans* model. For that purpose, transgenic nematodes expressing hVPS41 cDNAs were generated and crossed into isogenic lines of worms expressing both α-syn and GFP in DA neurons as described before (Hamamichi et al., 2008). Worms were scored as wild-type (WT) when all six anterior DA neurons were intact. Overexpression of α-syn alone resulted in significant degeneration in DA neurons (Fig. 1a). Strikingly, coexpression of hVPS41, either isoform 1 or isoform 2, significantly ameliorated DA neurodegeneration, both at days 7 and 10 post-hatching (Fig. 1a). Fig. 1b consists of two images whereby the top image displays a worm expressing only α-syn and GFP in the DA neurons where degeneration is observed in 3 of the 6 anterior DA neurons; in contrast, the lower image displays a worm coexpressing hVPS41, in addition to α-syn and GFP, this animal has all 6 anterior DA neurons intact.

To further investigate the neuroprotective properties of hVPS41 in vivo, we also examined the effect of hVPS41 expression in the worm model on vulnerability to 6-OHDA. Prior studies have demonstrated that 6-OHDA causes progressive and selective degeneration of *C. elegans* DA neurons (Nass et al., 2002; Cao et al., 2005). Transgenic animals expressing either isoform of hVPS41 were subjected to 6-OHDA treatment, as previously described (Nass et al., 2002; Cao et al., 2005). In control worms, 6-OHDA treatment resulted in substantial degeneration of DA neurons (Fig. 1c). Conversely, overexpression of either isoform of hVPS41 significantly rescued DA neurodegeneration, at all times tested following exposure (Fig. 1c). Fig. 1d shows the anterior DA neurons in *C. elegans* after exposure to 6-OHDA. The top image shows a worm expressing only GFP in the DA neurons and has 3 degenerating DA neurons, while the worm in the bottom image coexpresses hVPS41 with GFP and has the full complement of intact DA neurons.

Our experiments were performed in worm strains that have normal levels of endogenous CeVPS-41. Thus, the effect observed here may reflect the combined action of CeVPS-41 together with the induced expression of hVPS41. Worm strains that are null for *C. elegans vps-41* are maternal-effect embryonically lethal (Lackner et al., 2005), therefore it is not possible to generate homozygous *vps-41* knock-out worms that can be used for the overexpression of hVPS41 in a *C. elegans vps-41* null background.

Construction of SH-SY5Y neuroblastoma cell lines stably expressing hVPS41 protein

In order to evaluate the cellular role that VPS41 plays in neuronal cell death and possible underlying mechanisms, human neuroblastoma SH-SY5Y cells were stably transfected with constructs containing

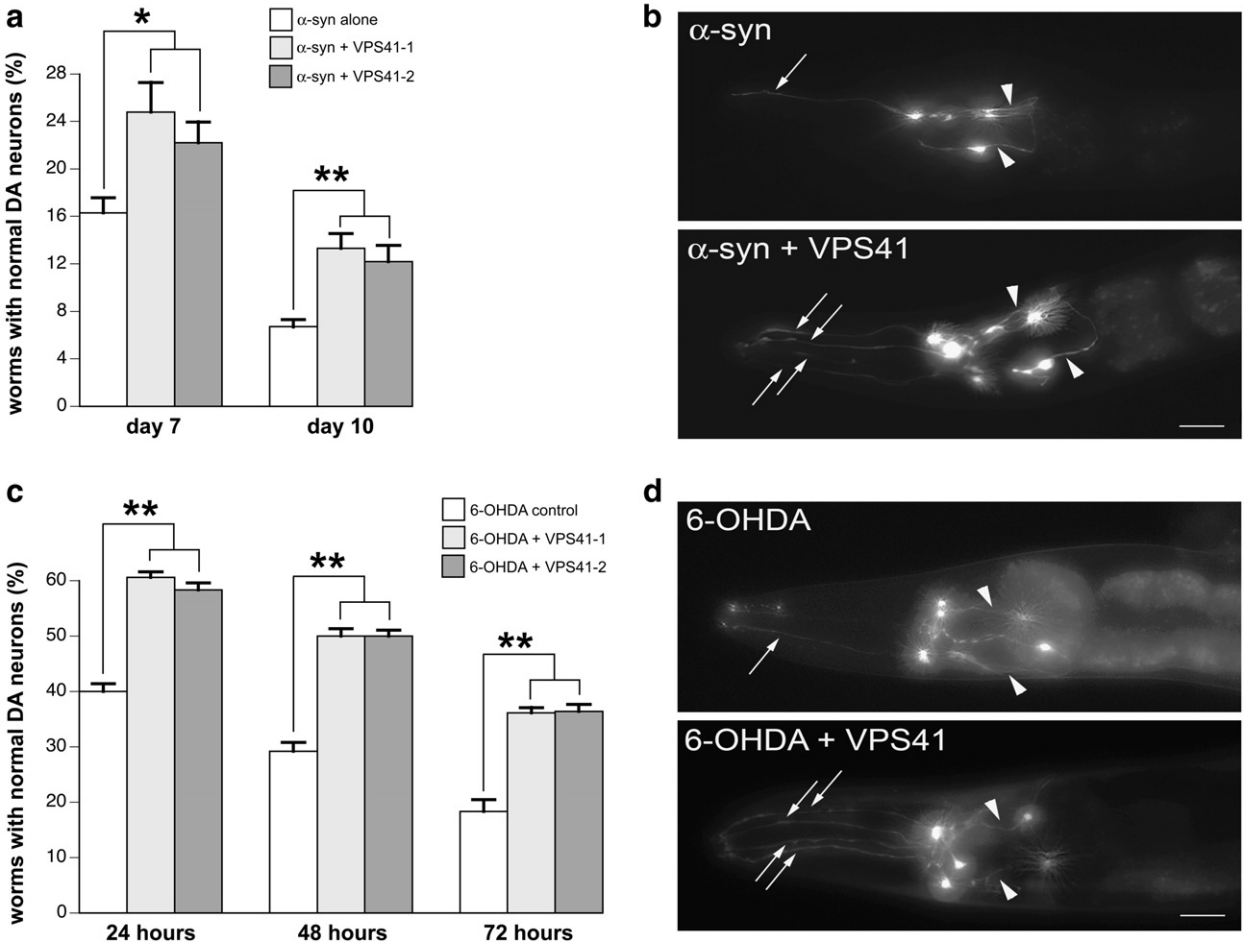

Fig. 1. Expression of either isoform of hVPS41 rescues DA neuron loss in *C. elegans*. Plasmids that drive the expression of different isoforms of hVPS41 were injected into *C. elegans*. After establishing stable lines, these transgenic animals were crossed into α-syn worms. The F2 homozygous progeny for both genes was synchronized and analyzed for protection from DA neurodegeneration at 7 and 10 days after hatching (a). Worms without any degeneration are considered to have normal DA neurons. Mean ± SD, $n = 270$ worms; $^{*}P<0.05$, $^{**}P<0.01$, Student's *t*-test. Panel b shows the anterior DA neurons of worms overexpressing α-syn alone or with hVPS41. The top image shows degeneration of 3 CEP type DA neurons, while the bottom image shows the full complement of anterior DA neurons when coexpressing hVPS41 with α-syn (b). Expression of either isoform of hVPS41 rescues DA neuron loss induced by 6-OHDA in *C. elegans* (c). Plasmids that drive the expression of different isoforms of hVPS41 were injected into *C. elegans*. After establishing stable lines, these worms were crossed into $P_{dat\text{-}1}$::GFP worms, subjected to 10 mM 6-OHDA for 1 hour, and analyzed for degeneration at 24, 48, and 72 hours post-treatment. Worms without visible degeneration are considered to have normal DA neurons. Mean ± SD, $n = 270$ worms; $^{*}P<0.05$, $^{**}P<0.01$, Student's *t*-test. Panel d shows anterior DA neurons in *C. elegans* after treatment with 6-OHDA. Top image is of a control worm expressing only GFP in the DA neurons and has degeneration in 3 CEP type DA neurons. In contrast, the bottom image is of a worm coexpressing hVPS41 and GFP in the DA neurons and does not exhibit any degeneration (a normal worm has 6 anterior DA neurons) after 6-OHDA treatment. Arrows depict CEP type DA neuronal processes while arrowheads depict ADE type DA neuronal processes.

hVPS41 cDNAs encoding either isoform 1 or isoform 2. Since no reliable hVPS41 antibody has been identified so far, a vector encoding a C-terminal myc tag was used in these constructs for easy identification. Stable transfection with hVPS41 cDNA and subsequent subcloning resulted in significant VPS41 protein expression in SH-SY5Y cells, and these expression levels were compared using Western blot against myc. In Fig. 2a, the levels of VPS41 expression in several cell lines are shown. GADPH was used as protein loading control. We selected clones of SH-SY5Y cells overexpressing comparable protein levels of either hVPS41 isoform 1 or 2 for further study; these are referred to as hVPS41-1 and hVPS41-2, respectively, while vector only cells are referred to as the vector control. For some experiments indicated, multiple cell lines were used and a representative blot showing various protein expression levels in these cell lines is in Fig. 2b.

Overexpression of hVPS41 in SH-SY5Y cells ameliorates cell death in cellular models of PD

We studied the effect of hVPS41 overexpression in several neurotoxin-based cellular models of PD. Chronic exposure of rodents or non-human primates to rotenone, a mitochondria complex I inhibitor, has been shown to recapitulate many of the pathological, biochemical, and behavioral features of PD (Greenamyre et al., 2001). In dopaminergic cell lines, it has also been shown to lead to

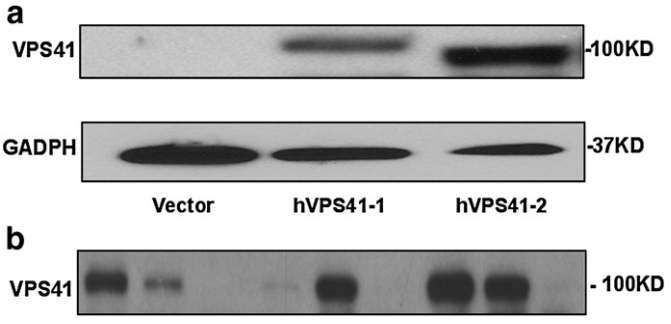

Fig. 2. Levels of hVPS41 protein expression in SH-SY5Y neuroblastoma cells stably transfected with hVPS41. (a) Representative immunoblot showing the expression of hVPS41 in the two cell lines used for the majority of the experiments described in this study. (b) Representative immunoblot which illustrates a number of additional stably transfected cell lines, demonstrating variable levels of hVPS41 expression. Several of these additional lines were used in confirmatory studies, as indicated in the text.

aggregation of α-syn and gradual cell death (Sherer et al., 2002). We subjected hVPS41 transfected cell lines to rotenone treatment at various concentrations (ranging from 0.1 μM to 20 μM) for 40 hours and cell death was measured via calculating the percentage of the intracellular enzyme LDH released into the medium. Rotenone induced dose-dependent increases in cell death as measured by LDH release in all cell lines tested. We found that the overexpression of hVPS41, either isoform 1 and 2, resulted in the attenuation of rotenone-induced LDH release in SH-SY5Y cells (Fig. 3a). This effect was subsequently verified in several other hVPS41-overexpressing cell lines. Interestingly, the expression level of hVPS41, which varies in the different cell lines, was not clearly correlated with the extent of neuroprotection in the cell lines tested, suggesting that even modest hVPS41 expression was sufficient to confer protection (Fig. 3a). Meanwhile, we observed no difference between cell lines over-expressing isoform 1 and 2 of hVPS41, suggesting both isoforms share similar neuroprotective properties.

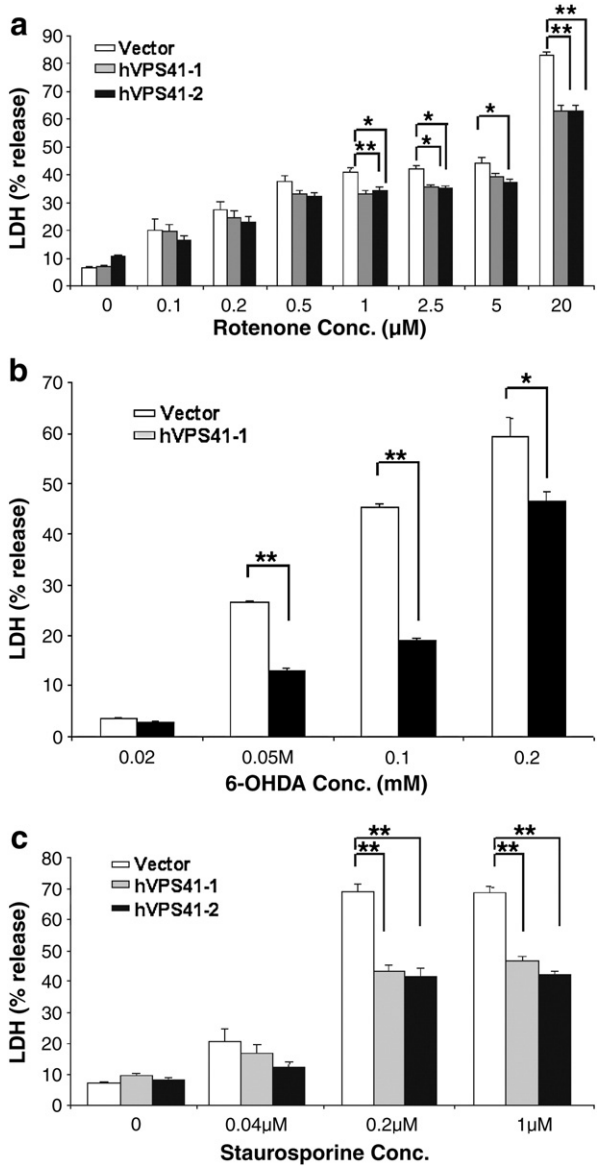

Fig. 3. Overexpression of hVPS41 in SH-SY5Y cells ameliorates cell death in cellular models of PD. (a) SH-SY5Y stable cell lines were treated with rotenone for 48 hours at indicated concentration, and cell death was measured by LDH release. (b) SH-SY5Y stable cell lines were treated with 6-OHDA for 16 hours at indicated concentration, and cell death was measured by LDH release. (c) SH-SY5Y stable cell lines were treated with staurosporine for 5 hours at indicated concentration, and cell death was measured by LDH release. $^{*}P<0.05$, $^{**}P<0.01$, Student's *t*-test. Mean ± SEM, $n=5$, ANOVA test from SigmaStat.

We also tested the effect of hVPS41 overexpression in SH-SY5Y cells in a second cellular model of PD, 6-OHDA toxicity (Blum et al., 2001). Cell lines expressing either empty vector or hVPS41-1 were subjected to 6-OHDA treatment for 16 hours, and cell death was measured via LDH assay. 6-OHDA induced dose-dependent increases in cell death as measured by LDH release in all cell lines tested. We found that overexpression of hVPS41-1 attenuated 6-OHDA-induced cell death in this model as well (Fig. 3b). We confirmed our result in the 6-OHDA model using an alternative assay for cell death, based on fluorescence of the dye calcein-AM. This dye, which accumulates intracellularly, fluoresces in response to increased cytosolic Ca^{+}, an early event in cell injury (Jonas, 2009). This approach also demonstrated a strong protective effect of hVPS41-1 against 6-OHDA treatment (data not shown).

In order to test whether the protection conferred by hVPS41 in SH-SY5Y cells also extends to other cell death models, we treated these cells with staurosporine, a general protein kinase inhibitor that has been used previously to induce cell death (Tamaoki et al., 1986). Stably transfected cell lines were subjected to staurosporine treatment for 5 hours and cell death was measured via LDH assay. The extent of staurosporine-induced cell death was also attenuated by expression of hVPS41 in SH-SY5Y cells (Fig. 3c).

hVPS41-1 expression does not prevent mitochondrial membrane depolarization in SH-SY5Y cells after rotenone treatment

Rotenone is an inhibitor of mitochondrial complex I and has been reported to induce mitochondrial membrane depolarization (Moon et al., 2005), which could lead to cell death (Kong et al., 2001; Recchioni et al., 2002). To investigate whether hVPS41 overexpression attenuates mitochondrial depolarization resulting from rotenone treatment, hVPS41-1 cell lines, as well as the vector control lines, were incubated in the absence or presence of rotenone, and mitochondrial membrane potential ($\Delta\psi_m$) was measured with the fluorometric dye JC-1. The ratio of JC-1 aggregates to monomer staining is independent of cell number or mitochondrial density, and thus can be used to quantitatively measure changes in $\Delta\psi_m$ (Chang et al., 2002). In all tested cell lines, rotenone induced a dose-dependent mitochondrial membrane depolarization as demonstrated by the decrease in the JC-1 ratio (Fig. 4). Interestingly, hVPS41 had no effect on mitochondrial membrane depolarization induced by rotenone treatment; the extent of JC-1 ratio decrease was similar among all cell lines treated, whether or not hVPS41 was overexpressed (Fig. 4). Similar effects were observed when cell lines were subjected to staurosporine treatment as the overexpression of hVPS41 also failed to alter the extent of mitochondrial membrane depolarization induced by that stressor (data not shown).

hVPS41-1 overexpression suppresses the activation of apoptosis induced by rotenone treatment in SH-SY5Y cells

Treatment with rotenone can result in the activation of mitochondrial-dependent apoptotic pathway (Potokar et al., 2006; Tada-Oikawa et al., 2003), which might contribute to the cell death in the pathogenesis of PD (Dauer and Przedborski, 2003). It has been shown that release of cytochrome *c* from the mitochondria results in the processing of pro-caspase-9 into its active fragment (Li et al., 1997), which subsequently converts pro-caspase-3 into its active form (Shi, 2002). Therefore, it is important to determine whether the neuroprotection displayed by hVPS41 is related to the inhibition of the apoptotic cell death pathway.

hVPS41-1 or vector control cells were incubated in the absence or presence of rotenone, and then lysed and immunoblotted to determine the presence of cleaved (active) caspase-9 or caspase-3.

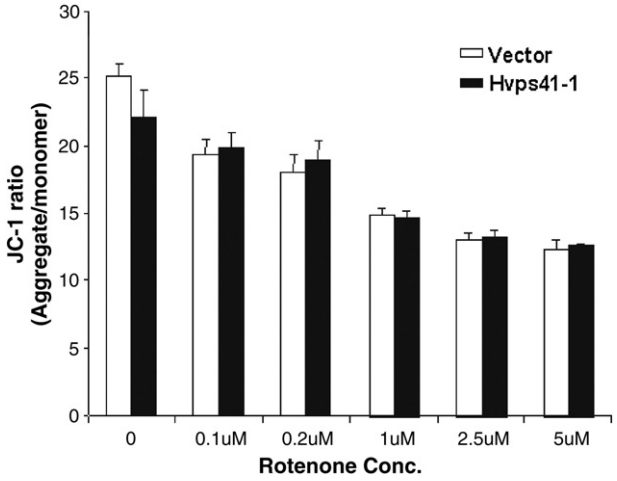

Fig. 4. hVPS41 overexpression does not prevent mitochondrial membrane depolarization in SH-SY5Y cells after rotenone treatment. SH-SY5Y stable cell lines were incubated under control conditions or in the presence of rotenone at indicated concentration for 48 hours and subsequently incubated with the mitochondrial membrane potential-sensitive dye JC-1, then quantitated with a fluorescence plate reader. There is no significant difference in mitochondrial membrane potential between vector cells and hVPS41-overexpressing lines, with or without rotenone treatment. Mean ± SD, $n = 3$ experiments.

Incubation of all these cell lines with rotenone resulted in the appearance of cleaved caspase-9 and caspase-3, indicating that apoptotic cascade was activated in our cellular model (Fig. 5a). The extent of caspase activation was, however, greatly reduced in hVPS41-1-overexpressing cells compared to that observed in vector control cells (Fig. 5a). We quantified this effect at a rotenone concentration of 0.5 μM (the concentration at which caspase-9 activation is maximal in both vector and hVPS41-overexpressing cell lines) and found that the protein level of activated caspase-9 in hVPS41-overexpressing cell lines was only 17.5 ± 12% of that in the vector control cells (mean ± SEM, $P<0.05$, $n = 3$).

Caspase-3 enzymatic activity was measured quantitatively using a fluorometric method in vector control and hVPS41-1 cell lines incubated in the absence or presence of rotenone. These results revealed that rotenone treatment resulted in an increase in caspase-3 enzymatic activity in both cell lines, but the extent of increase was significantly less in hVPS41-1 compared to vector control cell lines ($P<0.05$) (Fig. 5b).

We also tested the effect of hVPS41 overexpression on apoptosis induced by 6-OHDA as well as by staurosporine. We found that the overexpression of hVPS41 attenuates apoptosis in response to both of these toxins, as the extent of caspase activation was much less in the hVPS41-1 cells, when compared to the vector control cells (Figs. 5c and d).

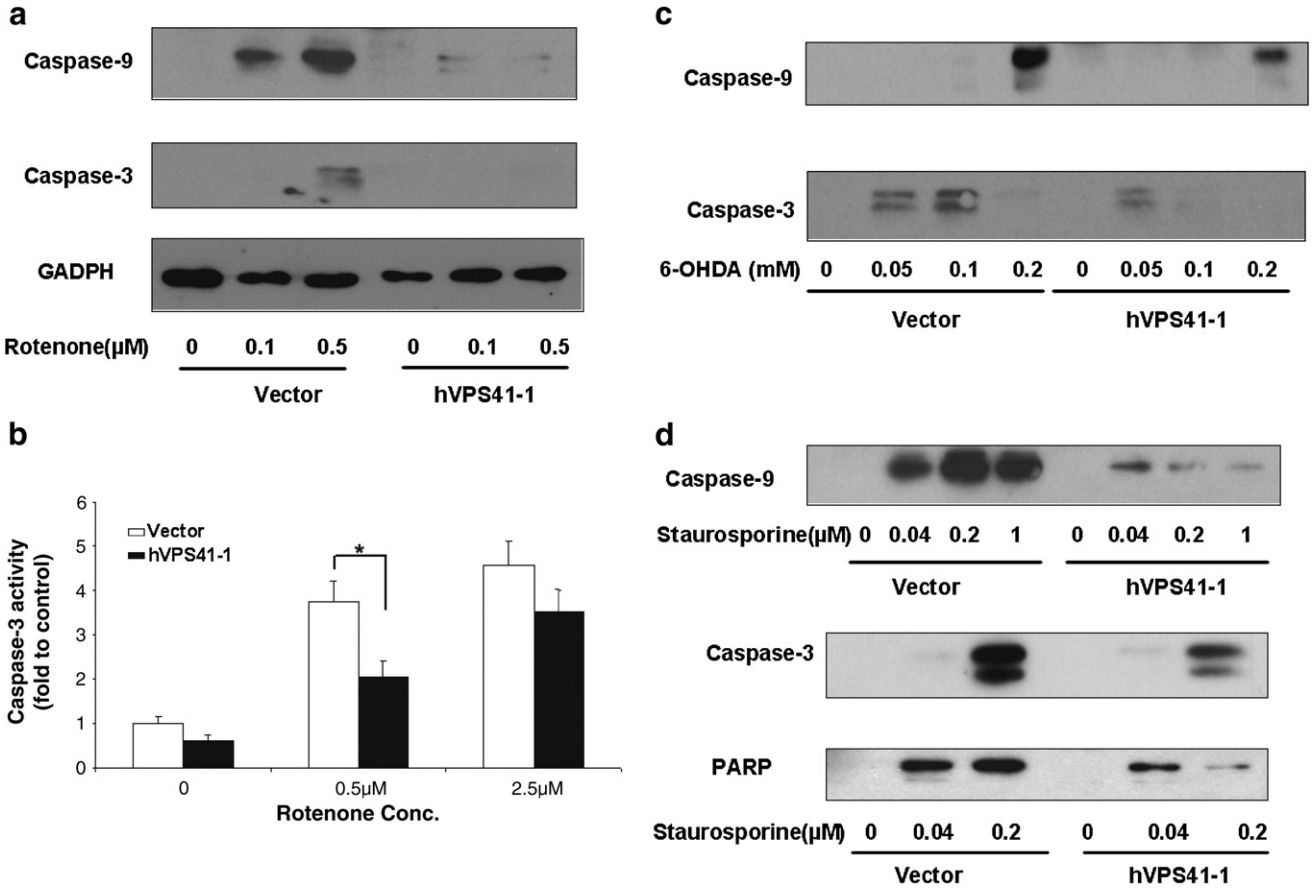

Fig. 5. hVPS41 overexpression suppresses the activation of apoptosis induced by rotenone treatment in SH-SY5Y cells. (a and b) Cells were incubated in the absence or in the presence of rotenone at the indicated concentrations for 48 hours prior to cell collecting. Immunoblots show that rotenone resulted in less pronounced caspase-9 and caspase-3 activation in hVPS41-overexpressing than in vector control cell lines. Measurement of caspase-3 activity assay revealed that overexpression of hVPS41-1 in SH-SY5Y cells attenuated caspase-3 activation induced by rotenone treatment. Data are expressed as fold increase over the activity in vector control cells under control conditions. Mean ± SEM. $n = 3$. $^{*}P<0.05$. (c) Cells were incubated in the absence or in the presence of 6-OHDA at the indicated concentrations for 6 hours prior to cell collecting, and immunoblots showed that rotenone resulted in less pronounced caspase-9 and caspase-3 activation in hVPS41-overexpressing than in vector control cell lines. (d) Cells were incubated in the absence or in the presence of staurosporine at the indicated concentrations for 6 hours prior to cell collecting, and immunoblots showed that staurosporine resulted in less pronounced caspase-9 and caspase-3 activation, as well as PARP cleavage in hVPS41-overexpressing than in vector control cell lines. Immunoblots shown are representative of three independent experiments.

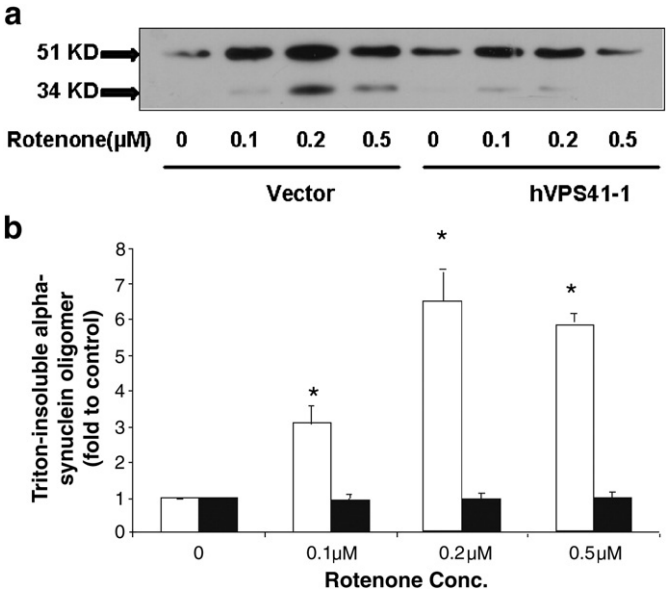

Fig. 6. hVPS41 overexpression modulates the change in α-syn solubility induced by rotenone treatment in SH-SY5Y cells. Cells were incubated in the absence or in the presence of rotenone at the indicated concentrations for 48 hours prior to cell collecting. These lysates were separated into Triton X-100-soluble and insoluble fractions. (a) Immunoblots show that rotenone treatment induced an increase in the abundance of Triton-insoluble component in vector control but not hVPS41-overexpressing cells. Immunoblots shown are representative of four independent experiments. Panel b summarizes the quantified result of four independent experiments as outlined in panel a. Mean ± SD, $n = 4$ experiments; $^{*}P < 0.05$, Student's *t*-test.

hVPS41-1 overexpression modulates the change in α-syn solubility induced by rotenone treatment in SH-SY5Y cells

Accumulation of detergent-insoluble high-molecular weight forms of α-syn is a characteristic of human synucleinopathies (Cantuti-Castelvetri et al., 2005; Goedert, 2001). In cellular model systems, rotenone treatment induces a similar accumulation of insoluble α-syn (Lee et al., 2004; Sherer et al., 2002). We used this approach to examine the effect of hVPS41 on the accumulation of Triton-insoluble α-syn in SH-SY5Y cells treated with rotenone. In agreement with previous studies, we found that rotenone treatment in vector control cell lines induced an increase in the abundance of Triton-insoluble protein which migrated predominantly with a size consistent with multimers (dimers and trimers) of α-syn, (Fig. 6). The increase in these insoluble forms ranged from 3- to 6-fold across the range of rotenone concentrations tested and was statistically significant at each of the concentrations studied. Interestingly, in hVPS41-overexpressing cells, the basal levels of Triton-insoluble α-syn were similar to vector cells, but the rotenone treatment paradigm failed to produce any significant increase in the abundance of Triton-insoluble α-syn (Figs. 6a and b). Triton-soluble forms of α-syn were similar in abundance in hVPS41 and control lines, and not affected by rotenone (not illustrated). We also examined cathepsin D, an essential lysosomal protein, and found that while the abundance of this protein was increased after treatment with rotenone, this effect was not altered in the presence of hVPS41 (data not shown).

Discussion

In this study, we have examined the potential neuroprotective effects of the expression of hVPS41, a protein related to lysosomal trafficking, in both invertebrate and cellular models of PD. We have found that overexpression of hVPS41, in both *C. elegans* and SH-SY5Y neuroblastoma cells, attenuates cell death induced by several stimuli that model the pathophysiology of PD: overexpression of α-syn and 6-OHDA treatment in *C. elegans*, and rotenone and 6-OHDA in SH-SY5Y cells. Our results demonstrate a consistent and strong neuroprotective effect in each of these model systems. In cellular systems, hVPS41 does not seem to modulate the loss of mitochondrial membrane potential ($\Delta\psi_m$) induced by these neurotoxins, but it does seem to modulate several downstream events in the apoptotic cascade. We also observed that the presence of hVPS41 reduced the accumulation of detergent-insoluble forms of α-syn after rotenone treatment, supporting a role for hVPS41 in the prevention of protein misfolding or the clearance of misfolded proteins. Collectively, these data suggest that hVPS41 may be a useful target of therapy in PD.

VPS41 was initially identified as a potential modulator of α-syn neurotoxicity in the *C. elegans* model system (Hamamichi et al., 2008). An important advantage of the *C. elegans* system is that screening and identification of potential neuroprotective factors are relatively rapid and efficient. A limitation, however, is that the results obtained in this invertebrate model may not be generalizable to more complex mammalian systems. Interestingly, several other targets initially identified in the same *C. elegans* system have proven to have protective properties in more complex models. These include two genes (PINK1 and DJ-1) which have been shown to cause autosomal recessive PD when deleted and a third gene (ULK2) recently identified in a whole-genome analysis of PD patient populations (Fung et al., 2006). In addition, the autophagy-associated gene ATG7, another target identified in this screen, has been functionally validated in mammals, as targeted disruption of this gene causes neurodegeneration in mice (Komatsu et al., 2006). We were able to observe protective effects of hVPS41 not only against α-syn, which was employed in the first phase of the *C. elegans* screen, but also against 6-OHDA and rotenone, two neurotoxins which are able to mimic many pathological hallmarks of PD, including neurodegeneration of DA neurons in substantia nigra and formation of structures similar to Lewy bodies (Blum et al., 2001; Bove et al., 2005; Uversky, 2004). These observations suggest that the *C. elegans* system has substantial predictive value with respect to effects in more complex organisms.

Our study provides insight into the mechanisms which may be responsible for the neuroprotective actions of hVPS41. Although both of the neurotoxins that we employed, 6-OHDA and rotenone, target the mitochondria, the overexpression of hVPS41 does not appear to alter the effect of the toxins on mitochondrial functions as measured using the JC-1 ratiometric dye. hVPS41 does, however, appear to block the activation of apoptotic mechanisms, with inhibition of activation of caspase-3 and caspase-9. hVPS41 was also able to attenuate cell death induced by staurosporine, which is commonly believed to be an general inducer of apoptosis (Lee et al., 2003). Apoptosis does seem to play a critical role in PD dopaminergic cell death (Dawson and Dawson, 2002). Increased levels of caspase-3 and BAX have been shown in nigral neurons in PD postmortem brain (Hartmann et al., 2001; Tatton, 2000). In adult mice, there is an up-regulation of BAX in the SNpc after MPTP administration and a decrease in Bcl-2, both of which are in parallel to MPTP-induced dopaminergic neurodegeneration (Vila et al., 2001). In human neural stem cells (hNSCs) and their differentiated cultures, rotenone was found to induce apoptosis, evidenced by ultrastructural characteristics and TUNEL staining. The time-dependent release of cytochrome *c*, apoptosis-inducing factor (AIF), and caspase 9/3-dependent apoptosis was also reported in that study (Li et al., 2005). Meanwhile, 6-OHDA infused in the striatum of adult rats induced the presence of apoptotic profiles, confirmed by electron microscopic studies (Marti et al., 2002). Intracellularly, 6-OHDA was also found to induce a caspase-3-dependent apoptotic cell death (Ding et al., 2004; Hanrott et al., 2006). Therefore, our results not only support a role for hVPS41 in protection against PD-relevant neurotoxins but also shed light on the underlying molecular mechanisms resulting in this neuroprotection.

While apoptosis seems to be part of the process of cell death in PD and models of the disease, the triggers for cell death in PD are less clear. α-Syn appears to have a central role: mutations of α-syn (Kruger et al., 2001; Kruger et al., 1998; Polymeropoulos et al., 1997), or even

overexpression of the normal protein as a result of gene multiplication (Ross et al., 2008; Singleton et al., 2003), cause dominantly inherited PD, while accumulation of aggregated α-syn in Lewy neuritis and Lewy bodies is a nearly universal feature of sporadic as well as genetic forms of the disease (Irizarry et al., 1998; Spillantini et al., 1997). Misfolding and accumulation of α-syn are observed in SH-SY5Y cells after treatment with rotenone (Sherer et al., 2003).

We found that the overexpression of hVPS41 markedly reduced the accumulation of detergent-insoluble high-molecular weight forms of α-syn. This suggests that a primary effect of hVPS41 may be to segregate and target for degradation misfolded α-syn, a role which is consistent with its known function in yeast (Bowers and Stevens, 2005). Our observations do not, of course, exclude the possibility of additional effects of hVPS41. We did not find any clear effect of VPS41 overexpression on the basal level of cathepsin D protein level or the induction of this protein by rotenone treatment, suggesting that enhanced VPS41 expression does not lead to an increased number of lysosomes, but it is certainly possible that hVPS41 may alter the functional properties of the lysosomal system. In yeast, VPS41 has an unusual role in mediating a pathway which bypasses the endosome and carries a small set of selected protein cargoes directly to the vacuole (Rehling et al., 1999). Whether a similar pathway is present in mammalian cells or whether VPS41 participates in the trafficking of a larger spectrum of proteins in mammals is presently uncertain. In either case, the view that enhanced trafficking of misfolded proteins is important for the actions of VPS41 is supported by recent work on related trafficking proteins, including Rab proteins, which lie upstream in the pathway between the Golgi and the lysosome, and also protects against α-syn toxicity in a variety of animal and cellular models of PD (Gitler et al., 2008).

It is important to note that the predictive value of all of the existing animal models with respect to human disease is at present uncertain. Indeed, the lack of any therapy proven efficacious in human PD is a barrier to rigorous validation of such model systems. Here, we have taken the approach of evaluating the actions of hVPS41 against neurodegeneration in several different classes of models, which encompass both genetic (α-syn) and neurotoxic approaches. As discussed elsewhere (Yacoubian and Standaert, 2009), success across several different models with diverse mechanisms conveys a higher probability of successful translation to human disease.

Two forms of VPS41 have been described in humans. Previous descriptions of these two isoforms, based on sequence analysis, suggested that they were likely to differ substantially in structure, with isoform 2 lacking the C-terminal RING-H2 sequence motif, which can be responsible for membrane association (McVey Ward et al., 2001). Careful analysis of the sequence reported, however, suggests that this conclusion was not correct. Using the sequence provided in the prior publication, we performed an independent alignment, which demonstrated that the predicted amino acid sequence difference was much less significant, with isoform 2 lacking only amino acids 83–107 in the amino terminus. This finding was also verified by direct sequence analysis of cDNA plasmids purchased from Origene and by our protein expression studies that showed an apparent size difference consistent with the N-terminal deletion. We also examined the properties of both human isoforms in our assays and found that they were similar, suggesting that the structural difference between hVPS41-1 and hVPS41-2 is not important for protection in models of PD.

In summary, our data support the neuroprotective efficacy of hVPS41 in a range of invertebrate and cellular models of PD. The protective effects appear to involve inhibition of apoptotic cascades. The mechanism of action is likely to involve enhancement of the clearance of abnormal high-molecular weight forms of α-syn, perhaps by targeting them to lysosomes for degradation. Further studies in intact mammalian models will be important to define the therapeutic potential of this target and may justify efforts to develop pharmacological strategies to induce the expression of VPS41 or to enhance its actions.

Acknowledgments

This work was supported by a *Target Validation 2007* award from the Michael J. Fox Foundation for Parkinson Research with assistance from the UAB Neuroscience Blueprint Core Center (NS57098).

References

Bandhyopadhyay, U., Cuervo, A.M., 2007. Chaperone-mediated autophagy in aging and neurodegeneration: lessons from alpha-synuclein. Exp. Gerontol. 42, 120–128.
Bijur, G.N., et al., 2000. Glycogen synthase kinase-3beta facilitates staurosporine-and heat shock-induced apoptosis. Protection by lithium. J. Biol. Chem. 275, 7583–7590.
Blum, D., et al., 2001. Molecular pathways involved in the neurotoxicity of 6-OHDA, dopamine and MPTP: contribution to the apoptotic theory in Parkinson's disease. Prog. Neurobiol. 65, 135–172.
Bove, J., et al., 2005. Toxin-induced models of Parkinson's disease. NeuroRx 2, 484–494.
Bowers, K., Stevens, T.H., 2005. Protein transport from the late Golgi to the vacuole in the yeast *Saccharomyces cerevisiae*. Biochim. Biophys. Acta 1744, 438–454.
Cantuti-Castelvetri, I., et al., 2005. Alpha-synuclein and chaperones in dementia with Lewy bodies. J. Neuropathol. Exp. Neurol. 64, 1058–1066.
Cao, S., et al., 2005. Torsin-mediated protection from cellular stress in the dopaminergic neurons of *Caenorhabditis elegans*. J. Neurosci. 25, 3801–3812.
Chang, L.K., et al., 2002. Mitochondrial involvement in the point of no return in neuronal apoptosis. Biochimie 84, 223–231.
Chu, Y., Kordower, J.H., 2007. Age-associated increases of alpha-synuclein in monkeys and humans are associated with nigrostriatal dopamine depletion: is this the target for Parkinson's disease? Neurobiol. Dis. 25, 134–149.
Cooper, A.A., et al., 2006. alpha-Synuclein blocks ER–Golgi traffic and Rab1 rescues neuron loss in Parkinson's models. Science 313, 324–328.
Cullen, V., et al., 2009. Cathepsin D expression level affects alpha-synuclein processing, aggregation, and toxicity in vivo. Mol. Brain 2, 5.
Dauer, W., Przedborski, S., 2003. Parkinson's disease: mechanisms and models. Neuron 39, 889–909.
Dawson, T.M., Dawson, V.L., 2002. Neuroprotective and neurorestorative strategies for Parkinson's disease. Nat. Neurosci. 5 Suppl., 1058–1061.
Decker, T., Lohmann-Matthes, M.L., 1988. A quick and simple method for the quantitation of lactate dehydrogenase release in measurements of cellular cytotoxicity and tumor necrosis factor (TNF) activity. J. Immunol. Methods 115, 61–69.
Ding, Y.M., et al., 2004. Effects of 6-hydroxydopamine on primary cultures of substantia nigra: specific damage to dopamine neurons and the impact of glial cell line-derived neurotrophic factor. J. Neurochem. 89, 776–787.
Finkbeiner, S., et al., 2006. Disease-modifying pathways in neurodegeneration. J. Neurosci. 26, 10349–10357.
Fung, H.C., et al., 2006. Analysis of the PINK1 gene in a cohort of patients with sporadic early-onset parkinsonism in Taiwan. Neurosci. Lett. 394, 33–36.
Gitler, A.D., et al., 2008. The Parkinson's disease protein alpha-synuclein disrupts cellular Rab homeostasis. Proc. Natl. Acad. Sci. U. S. A. 105, 145–150.
Gitler, A.D., et al., 2009. Alpha-synuclein is part of a diverse and highly conserved interaction network that includes PARK9 and manganese toxicity. Nat. Genet. 41 (3), 308–315.
Goedert, M., 2001. alpha-Synuclein and neurodegenerative diseases. Nat. Rev. Neurosci. 2, 492–501.
Greenamyre, J.T., et al., 2001. Complex I and Parkinson's disease. IUBMB Life 52, 135–141.
Hamamichi, S., et al., 2008. Hypothesis-based RNAi screening identifies neuroprotective genes in a Parkinson's disease model. Proc. Natl. Acad. Sci. U. S. A. 105 (2), 728–733.
Hanrott, K., et al., 2006. 6-Hydroxydopamine-induced apoptosis is mediated via extracellular auto-oxidation and caspase 3-dependent activation of protein kinase Cdelta. J. Biol. Chem. 281, 5373–5382.
Hartmann, A., et al., 2001. Is Bax a mitochondrial mediator in apoptotic death of dopaminergic neurons in Parkinson's disease? J. Neurochem. 76, 1785–1793.
Irizarry, M.C., et al., 1998. Nigral and cortical Lewy bodies and dystrophic nigral neurites in Parkinson's disease and cortical Lewy body disease contain alpha-synuclein immunoreactivity. J. Neuropathol. Exp. Neurol. 57, 334–337.
Jonas, E.A., 2009. Molecular participants in mitochondrial cell death channel formation during neuronal ischemia. Exp. Neurol. 218, 203–212.
Komatsu, M., et al., 2006. Loss of autophagy in the central nervous system causes neurodegeneration in mice. Nature 441, 880–884.
Kong, C.W., et al., 2001. Leukocyte mitochondria depolarization and apoptosis in advanced heart failure: clinical correlations and effect of therapy. J. Am. Coll. Cardiol. 38, 1693–1700.
Kotzbauer, P.T., et al., 2004. Fibrillization of alpha-synuclein and tau in familial Parkinson's disease caused by the A53T alpha-synuclein mutation. Exp. Neurol. 187, 279–288.
Kruger, R., et al., 2001. Familial parkinsonism with synuclein pathology: clinical and PET studies of A30P mutation carriers. Neurology 56, 1355–1362.
Kruger, R., et al., 1998. Ala30Pro mutation in the gene encoding alpha-synuclein in Parkinson's disease. Nat. Genet. 18, 106–108.
Lackner, M.R., et al., 2005. Chemical genetics identifies Rab geranylgeranyl transferase as an apoptotic target of farnesyl transferase inhibitors. Cancer Cell. 7, 325–336.
Lang, A.E., Lozano, A.M., 1998. Parkinson's disease. First of two parts. N. Engl. J. Med. 339, 1044–1053.

Lee, M.W., et al., 2003. Caspase-3-mediated cleavage of Rad9 during apoptosis. Oncogene 22, 6340–6346.
Lee, H.J., et al., 2004. Clearance of alpha-synuclein oligomeric intermediates via the lysosomal degradation pathway. J. Neurosci. 24, 1888–1896.
Li, P., et al., 1997. Cytochrome *c* and dATP-dependent formation of Apaf-1/caspase-9 complex initiates an apoptotic protease cascade. Cell 91, 479–489.
Li, J., et al., 2005. Rotenone-induced caspase 9/3-independent and -dependent cell death in undifferentiated and differentiated human neural stem cells. J. Neurochem. 92, 462–476.
Marti, M.J., et al., 2002. Striatal 6-hydroxydopamine induces apoptosis of nigral neurons in the adult rat. Brain Res. 958, 185–191.
McVey Ward, D., et al., 2001. hVPS41 is expressed in multiple isoforms and can associate with vesicles through a RING-H2 finger motif. Exp. Cell. Res. 267, 126–134.
Moon, Y., et al., 2005. Mitochondrial membrane depolarization and the selective death of dopaminergic neurons by rotenone: protective effect of coenzyme Q10. J. Neurochem. 93, 1199–1208.
Nass, R., Blakely, R.D., 2003. The *Caenorhabditis elegans* dopaminergic system: opportunities for insights into dopamine transport and neurodegeneration. Annu. Rev. Pharmacol. Toxicol. 43, 521–544.
Nass, R., et al., 2002. Neurotoxin-induced degeneration of dopamine neurons in *Caenorhabditis elegans*. Proc. Natl. Acad. Sci. U. S. A. 99, 3264–3269.
Nicholls, D.G., Ward, M.W., 2000. Mitochondrial membrane potential and neuronal glutamate excitotoxicity: mortality and millivolts. Trends Neurosci. 23, 166–174.
Olanow, C.W., Tatton, W.G., 1999. Etiology and pathogenesis of Parkinson's disease. Annu. Rev. Neurosci. 22, 123–144.
Polymeropoulos, M.H., et al., 1997. Mutation in the alpha-synuclein gene identified in families with Parkinson's disease. Science 276, 2045–2047.
Potokar, M., et al., 2006. Subcellular localization of Apaf-1 in apoptotic rat pituitary cells. Am. J. Physiol. Cell. Physiol. 290, C672–677.
Qiao, L., et al., 2008. Lysosomal enzyme cathepsin D protects against alpha-synuclein aggregation and toxicity. Mol. Brain 1, 17.
Radisky, D.C., et al., 1997. Characterization of VPS41, a gene required for vacuolar trafficking and high-affinity iron transport in yeast. Proc. Natl. Acad. Sci. U. S. A. 94, 5662–5666.
Ramirez, A., et al., 2006. Hereditary parkinsonism with dementia is caused by mutations in ATP13A2, encoding a lysosomal type 5 P-type ATPase. Nat. Genet. 38, 1184–1191.
Recchioni, R., et al., 2002. Apoptosis in human aortic endothelial cells induced by hyperglycemic condition involves mitochondrial depolarization and is prevented by *N*-acetyl-L-cysteine. Metabolism 51, 1384–1388.
Rehling, P., et al., 1999. Formation of AP-3 transport intermediates requires Vps41 function. Nat. Cell. Biol. 1, 346–353.
Ross, O.A., et al., 2008. Genomic investigation of alpha-synuclein multiplication and parkinsonism. Ann. Neurol. 63, 743–750.
Sherer, T.B., et al., 2002. An in vitro model of Parkinson's disease: linking mitochondrial impairment to altered alpha-synuclein metabolism and oxidative damage. J. Neurosci. 22, 7006–7015.
Sherer, T.B., et al., 2003. Mechanism of toxicity in rotenone models of Parkinson's disease. J. Neurosci. 23, 10756–10764.
Shi, Y., 2002. Mechanisms of caspase activation and inhibition during apoptosis. Mol. Cell 9, 459–470.
Shin, Y., et al., 2005. The co-chaperone carboxyl terminus of Hsp70-interacting protein (CHIP) mediates alpha-synuclein degradation decisions between proteasomal and lysosomal pathways. J. Biol. Chem. 280, 23727–23734.
Singleton, A.B., et al., 2003. alpha-Synuclein locus triplication causes Parkinson's disease. Science 302, 841.
Smiley, S.T., et al., 1991. Intracellular heterogeneity in mitochondrial membrane potentials revealed by a J-aggregate-forming lipophilic cation JC-1. Proc. Natl. Acad. Sci. U. S. A. 88, 3671–3675.
Spillantini, M.G., et al., 1997. alpha-Synuclein in Lewy bodies. Nature 388, 839–840.
Tada-Oikawa, S., et al., 2003. Mechanism for generation of hydrogen peroxide and change of mitochondrial membrane potential during rotenone-induced apoptosis. Life Sci. 73, 3277–3288.
Tamaoki, T., et al., 1986. Staurosporine, a potent inhibitor of phospholipid/Ca^{++} dependent protein kinase. Biochem. Biophys. Res. Commun. 135, 397–402.
Tatton, N.A., 2000. Increased caspase 3 and Bax immunoreactivity accompany nuclear GAPDH translocation and neuronal apoptosis in Parkinson's disease. Exp. Neurol. 166, 29–43.
Uversky, V.N., 2004. Neurotoxicant-induced animal models of Parkinson's disease: understanding the role of rotenone, maneb and paraquat in neurodegeneration. Cell. Tissue Res. 318, 225–241.
Vila, M., et al., 2001. Bax ablation prevents dopaminergic neurodegeneration in the 1-methyl-4-phenyl-1,2,3,6-tetrahydropyridine mouse model of Parkinson's disease. Proc. Natl. Acad. Sci. U. S. A. 98, 2837–2842.
Yacoubian, T.A., Standaert, D.G., 2009. Targets for neuroprotection in Parkinson's disease. Biochim. Biophys. Acta 1792 (7), 676–687.